

REPORT DOCUMENTATION PAGE				Form Approved OMB No. 0704-0188	
Public reporting burden for this collection of information is estimated to average 1 hour per response, including the time for reviewing instructions, searching existing data sources, gathering and maintaining the data needed, and completing and reviewing this collection of information. Send comments regarding this burden estimate or any other aspect of this collection of information, including suggestions for reducing this burden to Department of Defense, Washington Headquarters Services, Directorate for Information Operations and Reports (0704-0188), 1215 Jefferson Davis Highway, Suite 1204, Arlington, VA 22202-4302. Respondents should be aware that notwithstanding any other provision of law, no person shall be subject to any penalty for failing to comply with a collection of information if it does not display a currently valid OMB control number. PLEASE DO NOT RETURN YOUR FORM TO THE ABOVE ADDRESS.					
1. REPORT DATE (DD-MM-YYYY) 03-03-2003		2. REPORT TYPE Technical Paper		3. DATES COVERED (From - To)	
4. TITLE AND SUBTITLE The Application of Fracture Mechanics to Estimate the Crack Length for Inspection				5a. CONTRACT NUMBER	
				5b. GRANT NUMBER	
				5c. PROGRAM ELEMENT NUMBER	
6. AUTHOR(S) C.T. Liu				5d. PROJECT NUMBER 2302	
				5e. TASK NUMBER 0378	
				5f. WORK UNIT NUMBER	
7. PERFORMING ORGANIZATION NAME(S) AND ADDRESS(ES) Air Force Research Laboratory (AFMC) AFRL/PRSM 10 E. Saturn Blvd. Edwards AFB, CA 93524-7680				8. PERFORMING ORGANIZATION REPORT NUMBER AFRL-PR-ED-TP-2003-057	
9. SPONSORING / MONITORING AGENCY NAME(S) AND ADDRESS(ES) Air Force Research Laboratory (AFMC) AFRL/PRS 5 Pollux Drive Edwards AFB CA 93524-7048				10. SPONSOR/MONITOR'S ACRONYM(S)	
				11. SPONSOR/MONITOR'S NUMBER(S) AFRL-PR-ED-TP-2003-057	
12. DISTRIBUTION / AVAILABILITY STATEMENT Approved for public release; distribution unlimited.					
13. SUPPLEMENTARY NOTES					
20030326 020					
14. ABSTRACT					
15. SUBJECT TERMS					
16. SECURITY CLASSIFICATION OF:			17. LIMITATION OF ABSTRACT	18. NUMBER OF PAGES	19a. NAME OF RESPONSIBLE PERSON Sheila Benner
a. REPORT Unclassified	b. ABSTRACT Unclassified	c. THIS PAGE Unclassified	A		19b. TELEPHONE NUMBER (include area code) (661) 275-5963

FILE

MEMORANDUM FOR PRS (In-House Publication)

FROM: PROI (STINFO)

05 Mar 2003

SUBJECT: Authorization for Release of Technical Information, Control Number: **AFRL-PR-ED-TP-2003-057**
55642 — C.T. Liu (AFRL/PRSM), "The Application of Fracture Mechanics to Estimate the Crack Length for
Inspection"

2003 ASME Pressure Vessel Conference
(Cleveland, OH, 20-24 July 2003) (Deadline: 21 Mar 2003)

(Statement A)

The Application of Fracture Mechanics to Predict the Critical Initial Crack Length

C. T. Liu
AFRL/PRSM
10 E. Saturn Blvd.
Edwards AFB CA 93524-7680

Abstract

In this study, a method is developed based on fracture mechanics, for predicting the equivalent critical initial crack size, a_{ic} in a particulate composite material. The predicted a_{ic} is the crack size that should be used to develop an inspection criterion to determine the reliability of a structure made of the particulate composite material.

Introduction

Reliable performance of a structure in critical applications depends on assuring that the structure in service satisfies the conditions assumed in design and life prediction analyses. Reliability assurance requires the availability of nondestructive testing and evaluation (NDE) techniques to characterize discrete cracks according to their location, size, and orientation. This leads to an improved assessment of the potential criticality of individual flaws. To achieve this goal, an inspection criterion, regarding the size of the crack and the inspection interval, needs to be developed. The inspection criterion should not be driven by inspection capability of NDE methods, but rather, the selection of NDE methods should be driven by real engineering requirements.

It is well known in the aerospace industry that the initial crack sizes in metals and super alloys are too small to be detected by any NDE techniques. Consequently, the initial crack size in metals has been determined using experimental results, such as fractographic data or S-N data. From the experimental S-N data, one can determine the critical crack size at the time of failure (1-2). Then, the initial crack size is computed from the critical crack size by conducting the crack growth analysis backward. After determining the initial crack size, fatigue failure of aircraft or aerospace structural components can be predicted under any service loading spectra by carrying out the crack growth analysis.

While the basic concept for determining the initial crack size in particulate composite materials is similar to that for metallic materials used in aircraft industry, there are significant differences in the technical approach. This is because the crack growth behavior in particulate composite materials under constant strain rate loading is quite different from that in metals or super alloys subjected to cyclic fatigue loading. Therefore, it is the purpose of this study to develop a technique to predict the initial crack size, which is used to develop the inspection criterion.

In this study, the equivalent critical initial crack size (ECICS) in a particulate composite material, containing hard particles embedded in a rubber matrix, was determined using constant strain rate crack propagation test data. Uniaxial tensile specimens with and without pre-cracks were tested at a constant strain rate of 0.04 in/in/min. The experimental data were used to develop a crack

DISTRIBUTION STATEMENT A
Approved for Public Release
Distribution Unlimited

growth model, which is a material property, and to validate the developed technique to predict the critical initial crack size. In addition, statistical methods were used to determine the statistical distribution function of the critical initial crack size.

Analytical Analysis

To determine the ECICS, the following information is needed: (1) crack growth rate parameters, (2) critical stress intensity K_{IC} and threshold stress intensity factor K_{th} below which crack will not grow, and (3) time to failure data under a constant strain rate loading condition. Crack growth rate parameters as well as K_{IC} and K_{th} are determined experimentally using pre-flawed specimens. Time to failure data is also obtained experimentally using specimens without a pre-crack.

For pre-cracked specimens, the stress intensity factor K_I is given by

$$K_I = \sigma (\pi a)^{1/2} f(a/w) \quad (1)$$

In which, σ is the applied stress, $f(a/w)$ is the geometric correction factor, a is the crack length, and w is the width of the specimen. The functional relationship between $f(a/w)$ and a/w is shown below.

$$f(a/w) = 0.5854(a/w)^3 + 1.099(a/w)^2 + 0.8672(a/w) + 1.049 \quad (2)$$

For a specimen subject to a constant strain rate, the stress intensity factor K_I reaches the critical stress intensity factor K_{IC} at the instant of fracture, and the corresponding flaw size is denoted by a_c , referred to as the critical flaw size or the terminal flaw size. It follows from Eq. (1) that

$$K_{IC} = \sigma_c (\pi a_c)^{1/2} f(a_c/w) \quad (3)$$

Where σ_c is the critical stress at fracture.

The crack growth rate da/dt has been shown to be a power function of the stress intensity factor K_I , i.e.,

$$da/dt = Q K_I^m \quad (4)$$

in which m and Q are crack growth rate parameters. Experimental findings, obtained from a different program, reveal that Q and m are material constants, because they are insensitive to the specimen's thickness and geometry.

When a specimen without pre-crack is subjected to a constant rate, the entire loading history and hence the stress history $\sigma = \sigma(t)$ can be measured, including the critical stress σ_c at the time of fracture, t_c . For a given critical stress intensity factor K_{IC} (material constant), the critical flaw size a_c can be computed from Eq. (3). Consequently, the initial flaw size a_0 at $t=0$ can be obtained by integrating Eq. (4), based on the terminal condition (a_c, t_c) and the stress history $\sigma(t)$.

Experimental Analysis

In this study, two series of constant strain rate tests were conducted. In the first series of tests, uniaxial specimens without a pre-crack were tested at a constant strain rate of 0.04 min^{-1} (3). The specimen's dimensions are 0.375 in. wide, 2.75 in. height. The thicknesses of the specimens are .2 in., 0.5 in., 1.0 in., and 1.5 in. The second series of constant strain rate tests were conducted on specimens with and without pre-crack at four different strain rates, 0.067 min^{-1} , 0.67 min^{-1} , 6.7 min^{-1} , and 66.7 min^{-1} . The dimensions of the pre-cracked specimen are 1.0 in. wide, 3.0 in. height, and 0.2 in. thick. For the pre-cracked specimen, a single edge-crack was cut at the edge of the specimen using a razor blade. Three different pre-crack sizes, 0.1 in., 0.2 in., and 0.3 in., were considered. The results of the second series of tests were used to develop a crack growth model and to verify the estimated equivalent critical initial crack sizes (ECICS).

Test results for the stress history $\sigma(t)$ of each specimen under constant strain rate have been recorded. The time to fracture, t_c , which corresponds to the maximum $\sigma(t)$, i.e., $\sigma(t_c) = \max \sigma(t)$, can be determined. Then, the critical crack size a_c corresponding to t_c is computed from Eq. (3) for a given K_{IC} where $\sigma_c = \sigma(t_c)$. With the terminal condition (t_c, a_c) Eq. (4) is used to perform the crack growth analysis backward to obtain the crack growth curve $a(t)$ from t_c to 0. The crack growth parameters Q and m in Eq. (4) were determined from crack propagation test results using pre-cracked specimens. Finally, from the stress history $\sigma(t)$ and the crack growth curve $a(t)$, the stress intensity factor time histories $K_I(t)$ can be determined.

Constant strain rate tests were conducted on specimens with and without pre-cracks at a strain rate of 0.04 in/in/min (3). The critical stress σ_c and the time to failure t_c were determined from the specimen without pre-crack. The crack growth parameters m and Q were determined from the specimens with pre-flaw. The results are: $m = 2.084$ and $Q = 9.3325 \times 10^{-7}$ in which the units are force in pound, length in inch, and time in minute. Further, the critical stress intensity factor and the threshold stress intensity factor are $78.3 \text{ psi (in)}^{1/2}$ and $52 \text{ psi (in)}^{1/2}$, respectively.

In the crack growth analysis to obtain the crack growth curve $a(t)$, the effect of the threshold stress intensity factor for the onset of crack growth, K_{th} , was not considered. Hence, the flaw size, a_0 , at time $t = 0$ represents the equivalent critical initial flaw sizes (ECIFS) with $K_{th} = 0$. By knowing K_{th} , the time t^* corresponding to K_{th} can be obtained from the $K_I(t)$ versus t plot, and, similarly, the crack size at t^* , denoted by a^* , can be obtained from the $a(t)$ versus t plot.

Results and Discussion

The effect of specimen thickness on the initial flaw size and the critical flaw size were investigated. The results of analyses show that for specimen thicknesses equal to 0.2 in., 0.5 in., and 1.0 in., the variations among a_0 and a_c are small and the average values a_0 and a_c are 0.126 in. and 0.132 in., respectively. For specimen thickness equal to 1.5 in. the average values of a_0 and a_c are 0.144 in. and 0.158 in., respectively, and they are 14% and 20% higher when the specimen thickness is equal to or less than 1.0 in. The increase in a_0 and a_c in thicker specimen is probably due to the size effect of this material. Unlike the brittle metallic materials, this high toughness particulate composite material shows higher strength when the size of the specimen is increased.

The size effect of this material is a subject of further research. Considering the highly nonhomogeneous nature of the highly filled particulate composite and for the engineering application purpose, it is reasonable to assume that a_0 and a_c are independent of the specimen thickness. Under this assumption, the average value and the coefficient of variation of a_0 (a_c) are 0.1308 in. (0.1462 in.) and 0.0092 (0.0079), respectively.

The results of the analyses show that a_0 , a^* , a_c vary from specimen to specimen. Hence, the statistical analyses of these quantities have been conducted. The distribution of the equivalent initial crack size provides information for determining the threshold crack size for nondestructive inspection. In this study, four statistical distribution functions: (i) normal distribution, (ii) Lognormal distribution, (iii) two-parameter Weibull distribution, and (iv) second asymptotic distribution of maximum value, have been considered. These distribution functions are given as follows

$$F_X(x) = \Phi\left(\frac{x - u}{\sigma}\right) \quad (5)$$

$$F_X(x) = \Phi\left(\frac{\ln x - u^*}{\sigma^*}\right) \quad (6)$$

$$F_X(x) = 1 - \exp[-(x/\beta)^\alpha] \quad (7)$$

$$F_X(x) = \exp[-(x/v)^{-\kappa}] \quad (8)$$

in which $F_X(x) = P[X \leq x]$ is the distribution function of the random variable X ; u and σ are the mean and standard deviation of X ; Φ is the standard normal distribution function; μ^* and σ^* are the mean and standard deviation of $\ln X$; α and β are the shape parameter and scale parameter of the Weibull distribution; and κ and v are the distribution parameters of the second asymptotic distribution of maximum value. Parameters u , σ , u^* , σ^* were obtained using the method of moment, whereas α , β , κ and v were determined using the probability plot. A summary of the statistical parameters of different statistical distribution functions is shown in Table 1. The goodness of fit for all distributions above has been conducted using the Kolomogorov-Smirov test. Due to small statistical dispersion of data sets, test results indicate that all the distribution functions are acceptable at a high level of significance, although the second asymptotic distribution of maximum value fits both data sets slightly better.

A typical plot of the statistical distribution of the second asymptotic distribution of maximum value for a_0 is shown in Fig. 1. For a comparison purpose, experimental data, shown as circles, are also included in these figures. It is seen that the second asymptotic distribution of maximum value fits the experimental data very well. In addition, the results of the goodness of fit analyses for different distributions indicate that the second asymptotic distribution of maximum value has the best fit for the distribution of a_0 .

For the assurance of the integrity and reliability of the structure in its design service life, large initial cracks are most critical. Hence, the upper tail portion of the distribution function of ECICS

is most important. Consequently, on the basis of experimental data, it is highly desirable to select a distribution function whose upper tail portion is conservative. To emphasize the importance of the upper tail distribution, we present the distribution of crack exceedance $F_X^*(x)$ as follows

$$F_X^*(x) = 1 - F_X(x) \quad (9)$$

in which $F_X^*(x) = P[X > x]$ is the complement of $F_X(x)$ indicating the probability that the random variable X (such as ECICS) is larger than a value x . $F_X^*(x)$ is referred to as the crack exceedance curve. A typical plot of the exceedance curves for Weibull distribution and the second asymptotic distribution of maximum value is shown in Fig.2. The exceedance curve can be used to determine the probability of exceed for a given crack length.

In this study, the equivalent critical initial crack is a predicted crack assumed to exist in the material. It characterizes the equivalent effect of an actual initial crack in the material. The equivalent initial crack is not a physically observable initial crack. Therefore, the predicted equivalent initial crack must be justified using applicable test data. In other words, the predicted ECICS needs to be verified experimentally. To achieve this goal, uniaxial edge-cracked tensile specimens with different initial crack lengths (0 in., 0.1 in., 0.2 in., and 0.3 in.) were tested at four different strain rates (0.067 in/in/min, 0.67 in/in/min, 6.67 in/in/min, and 66.7 in/in/min). The tests results, plotting the maximum stress, σ_{max} , versus the corresponding time, t_{max} , are shown in Fig.3. By shifting the un-precracked specimen data vertically downward until they superpose upon those of the pre-cracked specimen, we can obtain an estimate for the initial flaw size in the un-precracked specimen. The dashed lines in Fig.3 represent the vertically shifted curves. According to Fig.3, the initial crack size in the un-precracked specimen is approximately equal to 0.1 in., which compares well with the predicted value of 0.1308 in. This indicates that the accuracy of the crack growth model and the developed ECICS predictive model are excellent.

Conclusion

In this study, a method is developed to predict the equivalent critical initial crack length and its statistical distribution function of a particulate composite material. The validity of the developed method has been verified. The results of analyses indicate that the equivalent critical initial crack size follows the second asymptotic distribution of maximum value. The predicted equivalent critical initial crack size is the size of the crack that needs to be detected by nondestructive testing techniques and it should be used to develop the inspection criterion.

References

- (1) Yang, J.N., Manning, S.D., Rudd, J.L., and Bader, R.M. (1995), "Investigation of Mechanistic-Based Equivalent Initial Flaw Size Distribution," Proceeding of the 18th Symposium of ICAF, Melbourne, Australia, 385-403.

(2) Yang, J.N., Manning, S.D., and Newman, J.C., Jr., (1997), "Equivalent Initial Flaw Size Distribution for Notches in 2024-T3 Aluminum, Accounting for Short Crack Effect," Proceeding of 1997 International Conference on Structural Safety and Reliability, Kyoto, Japan.

(3) Liu, C. T. Unpublished data.

	a_0	a^*	a_c
u	0.1308	0.1344	0.1462
σ	0.0092	0.0090	0.0079
u^*	-2.037	-2.0092	-1.9242
σ^*	0.07021	0.06692	0.053961
α	17.5546	18.4513	23.0450
β	0.1348	0.1383	0.1497
k	13.2524	13.8081	17.1205
v	0.1258	0.1295	0.1419

Table1. Statistical Parameters of Different Statistical Distribution Functions.

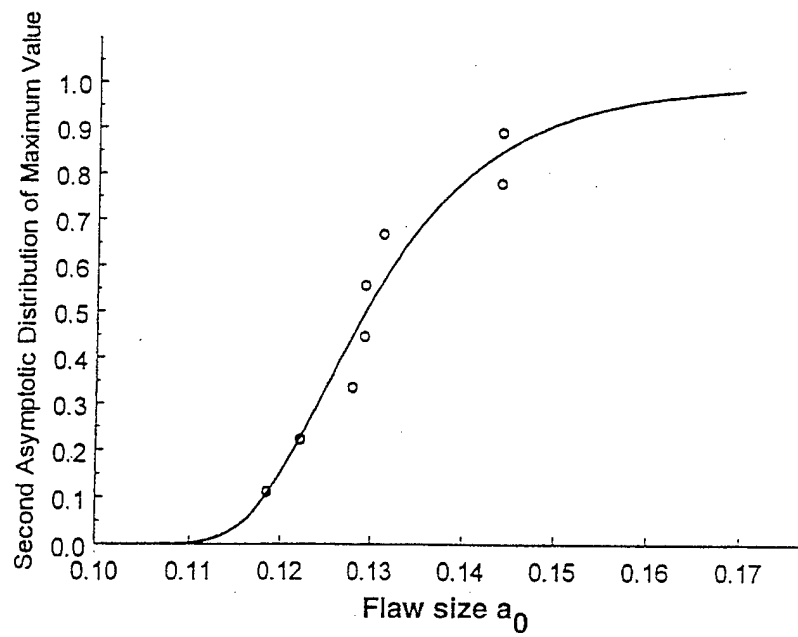


Fig. 1 Second Asymptotic Distribution of the Maximum Value Plot of a_0 .

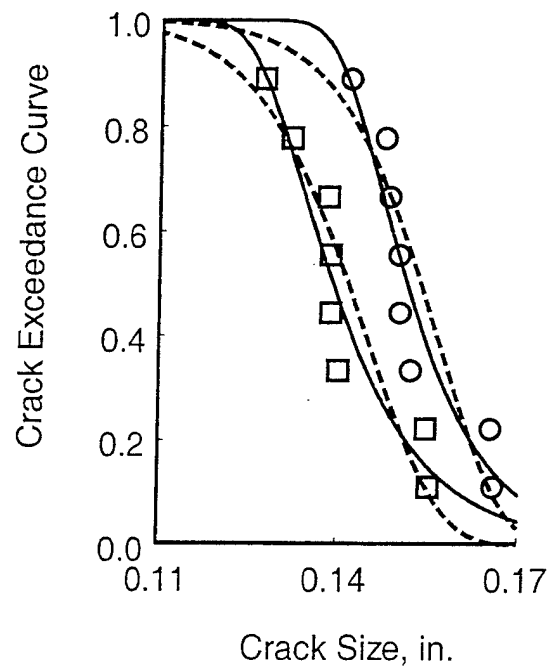


Fig. 2. Crack Exceedance Curves for a_0 (\square) and a_c (O); Solid Curves for Second Asymptotic Distribution of the Maximum Value and Dashed Curves for Weibull Distribution.

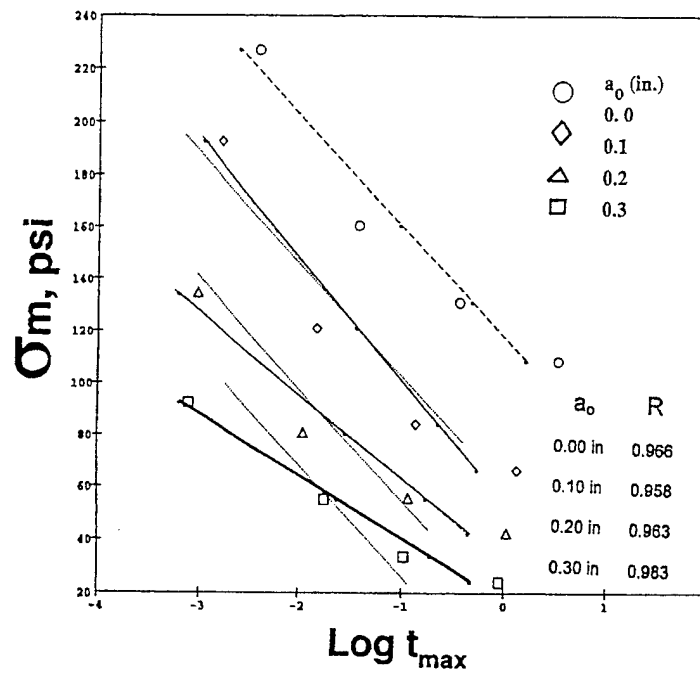


Fig. 3. Plot of Maximum Stress versus Maximum Time